

Electronic structure of the Si(111):GaSe van der Waals-like surface termination

Reiner Rudolph[†] Christian Pettenkofer[†], Aaron A. Bostwick^{‡||}, Jonathan A. Adams^{‡¶}, Marjorie A. Olmstead[‡] Bengt Jaeckel[§] Andreas Klein[§] and Wolfram Jaegermann[§]

[†] Hahn-Meitner-Institut, Solar Energy Research - SE6, Glienicker Strasse 100, 14109 Berlin, Germany

[‡] University of Washington, Department of Physics, Box 351560, Seattle, Washington 98195-1560, USA

[§] Darmstadt University of Technology, Department of Materials Science, Surface Science Division, Petersenstrasse 23, D-64287 Darmstadt, Germany

E-mail: olmstd@u.washington.edu

E-mail: aklein@surface.tu-darmstadt.de

Abstract. The electronic structure of the Si(111):GaSe van der Waals-like surface termination has been determined by angle-resolved photoelectron spectroscopy using photons in the energy range $h\nu = 12 - 170$ eV supplied by the BESSY and ALS synchrotron light sources. The Si(111):GaSe surface is isoelectronic to the passivated Si(111):H and Si(111):As surfaces, and also reflects the principal building block of layered chalcogenide GaSe single crystals. The electronic structure is discussed in relation to these systems. The chemical bond between the Si and Ga surface atoms is non-polar and therefore similar to the Ga-Ga bond in GaSe single crystals and also to the Si-Si bond in bulk silicon. This explains both the absence of a surface core-level shift in Si 2p photoelectron spectra of the terminated surface and the striking similarity between its observed band structure and that of bulk GaSe.

^{||} present address: Advanced Light Source, Berkeley

[¶] present address: Advanced Portfolio Technologies, London

1. Introduction

Silicon forms the backbone of modern microelectronics. However, its indirect band gap precludes widespread use in optoelectronic applications. Integration of commonly used optoelectronic materials into silicon technology is hindered by the large lattice and chemical mismatch between Si and III-V or II-VI semiconductors such as GaAs, InAs or ZnSe. Direct incorporation of these materials into silicon-based devices through heteroepitaxy will require development of suitable buffer layers to prevent interdiffusion and to relieve interface strain without creating optically active defects.

Van der Waals-epitaxy may provide ultrathin buffer layers for epitaxy of lattice mismatched materials [1, 2]. The first step is to establish a stable interface between Si and layered materials. The Si(111)/GaSe interface is the most intensively studied interface in van der Waals-epitaxy because the close matching between the Si(111) surface and bilayer building block of the layered GaSe crystal leads to a surface termination with outstanding properties. The van der Waals-surface termination formed by a Ga-Se bilayer, which corresponds to a half-sheet of the layered semiconductor GaSe, on Si(111) is extensively described in the literature [3, 4, 5, 6, 7, 8, 9, 10, 11, 12, 13, 14, 15]. It provides a chemically and electronically passivated Si surface, which is stable up to 500°C [11, 12, 14].

The bilayer termination of the Si(111) surface is isoelectronic to both H- and As-terminated Si, and the electronic structure resembles these, though with different interface dipoles between the bulk Si and the outermost surface layer. Alternatively, the electronic valence band structure of the surface may be described by an almost undisturbed GaSe band structure, where the Ga-Ga bond in the center of the layer is replaced by the interface Si-Ga bond, resulting in an almost one-to-one replacement of the corresponding energy levels. This establishes a non-polar Si-Ga bond in the Si(111):GaSe half-sheet van der Waals surface termination, which is also suggested by the absence of a surface core-level shift in the Si 2p spectra of the GaSe terminated surface [7, 12]. In combination with the chemical inertness and temperature stability of the surface, which is superior to the commonly used Si(111):H, the GaSe termination generates an exceptional surface to be used for Si based heterostructure devices.

In this contribution we report on determination of the electronic structure of the Si(111):GaSe surface termination using angle-resolved and energy-dependent valence band photoelectron spectroscopy and scanning tunneling spectroscopy. After a brief description of the experimental procedure (Sect. 2), the surface structure is reviewed (Sect. 3). The integrated surface electronic structure determined with scanning tunneling spectroscopy is presented in Sect. 4, followed by detailed band structure measurements with photoelectron spectroscopy in Sect. 5, where results are also presented for single crystal layered GaSe. Finally, in Sect. 6, we present a phenomenological model of the electronic structure of the surface based on molecular orbital considerations and the bulk GaSe band structure, and compare our results with the isoelectronic Si(111):H and Si(111):As surfaces.

2. Experimental

The Si(111):GaSe termination layer can be prepared in different ways. Either hydrogen terminated Si(111)- 1×1 :H surfaces or clean Si(111)- 7×7 surfaces may be used as a substrate. GaSe deposition may be either performed by separate evaporation of Ga and Se [12, 13], or by direct evaporation of the GaSe compound [6, 7, 15]. The GaSe surface termination layer is stable up to substrate temperatures of $\sim 550^\circ\text{C}$, whereas GaSe multilayer growth occurs only for $T \lesssim 500^\circ\text{C}$. Therefore high quality, nearly defect-free termination layers can be formed for intermediate temperatures. The quality of the obtained surfaces was checked by low-energy electron diffraction (LEED), which exhibit clear three-fold diffraction patterns with a low background level.

Photoelectron spectra were partly recorded at the TGM 7 beamline of the electron storage ring BESSY in Berlin, Germany, supplying linearly polarized light with photon energies ranging from 11 – 120 eV. A VG ADES 500 spectrometer with an acceptance angle of $\pm 2^\circ$ was used. The overall energy resolution of the setup was below 150 meV for photon energies below 40 eV and 350 meV at $h\nu = 80$ eV. Angular scans were performed by rotating the analyzer in the plane of light polarization (axis of rotation perpendicular to the plane containing the polarization vector, the photon propagation and the electron emission). The angle between the surface normal and incoming photons was set to 45° . Samples were prepared by selenization of monolayer Ga terminated Si(111) surfaces. The termination and surface quality was checked by LEED.

Additional measurements were taken at Beamline 7.0.1 at the Advanced Light Source (ALS) in Berkeley, CA, and at the University of Washington (UW) in Seattle, WA. These samples were prepared using a GaSe compound source; a few samples had supplemental Se from an electrochemical source to reduce Ga-terminated regions, which may be observed with STM [15] and result in a metallic component in Ga $3d$ spectra [16]. At UW, photoelectrons were excited by an unpolarized He resonance lamp with photon energy $h\nu = 21.2$ eV and detected by a Leybold EA-11 hemispherical analyzer (angle resolution $\pm 1 - 2^\circ$ at an angle of 55° from the photons. The sample was rotated on an axis perpendicular to plane defined by the photon and electron beams. At the ALS, horizontally polarized photons of energy $70 \leq 170$ eV were incident at an angle of 60° from the horizontally emitted electrons; the electrons were detected by a 137-mm Perkin-Elmer Omni IV hemispherical analyzer with angle resolution better than 1° . The sample was rotated about a horizontal axis lying in the plane containing the polarization and electron emission direction (*i.e.*, perpendicular to that at BESSY or UW).

3. Structure of the Si(111):GaSe surface

The structure of the Si(111):GaSe surface termination was determined by the group of Eddrief in 1997 using grazing incidence X-ray diffraction [4] and X-ray standing waves [5], and later also confirmed by photoelectron diffraction [6, 7] and atomic resolution scanning tunneling microscopy [15]. The structure of the surface is shown in Figure 1.

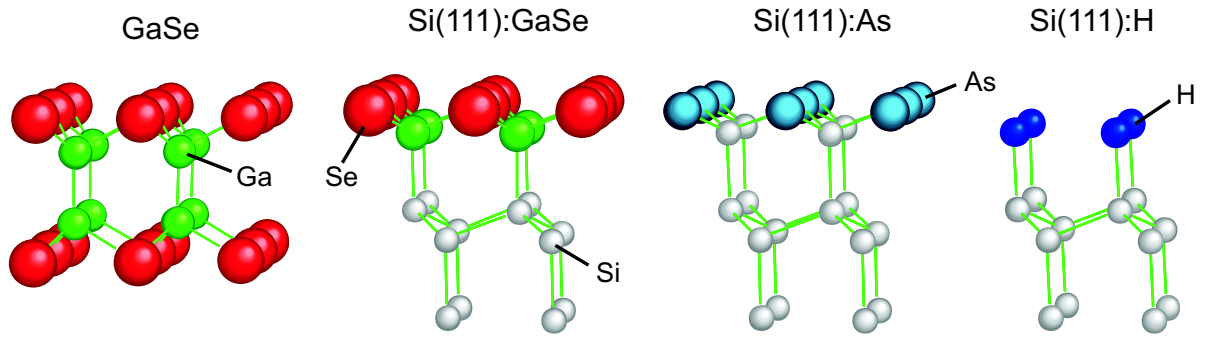


Figure 1. Structure of the Si(111):GaSe surface according to Refs. [4, 5] compared to a single GaSe layer. All chemical bonds are saturated, leading to a passivated surface. The surface is isoelectronic to the more common passivations Si(111):H and Si(111):As (below)

The surface is basically identical to that of the van der Waals surface of bulk layered GaSe. It is characterized by a layer of Ga between the topmost Si atoms and an outermost Se layer [4, 5, 6, 7]. Each Si atom binds to one Ga atom, while each Ga has one Si (below) and three Se (above) bonding partners. Each Se atom binds to three Ga atoms and has a doubly occupied lone pair orbital. The three Ga valence electrons are shared with the selenium ($2/3$ per bond) and Si (1 per bond). Four of six Se valence electrons are shared with Ga ($4/3$ per bond). The remaining two Se valence electrons occupy a lone pair orbital. The electron counting rule [17] is fulfilled and all chemical bonds are saturated. The Ga-Se surface layer has a structure essentially identical to that obtained by cutting the Se-Ga-Ga-Se unit layer of GaSe single crystals at the Ga-Ga bond. A hypothetical cut half-sheet layer of GaSe has an hexagonal array of singly occupied Ga dangling bond orbitals with a lattice constant of 3.74 \AA , which matches closely to an unreconstructed Si(111) surface with a surface atom distance of $\sqrt{2}/2 \cdot 5.43 \text{ \AA} = 3.84 \text{ \AA}$.

On the other hand, the surface may also be viewed as isoelectronic to Si(111):H and Si(111):As. The surface bilayer of ideally-terminated Si(111) has 8 valence electrons per Si pair; seven are in bonds with other Si atoms, and a single electron occupies the surface dangling bond. Addition of hydrogen, with its single electron, saturates this dangling bond and brings the dangling bond orbital well below the valence band maximum [18, 19], passivating the surface. Replacement of the top Si and H by an arsenic atom, with 5 valence electrons, likewise leaves the surface passivated with a doubly-occupied lone-pair and three Si-As bonds. The electronic structure is similar to Si(111):H, except that the large charge transfer between the Si and As results both in a large (0.75 eV) core-level shift on the interface Si 2p [20] and the lone-pair state lies about 3 eV closer to the Si valence band maximum [21] than does the Si-H bond. Exchanging the Si-As bilayer with a Ga-Se bilayer again results in the same number of valence electrons and a passivated surface with a doubly-occupied lone pair surface orbital. As discussed below, the reduced surface dipole of Si(111):GaSe lowers the energy of the lone-pair orbital relative to Si(111):As.

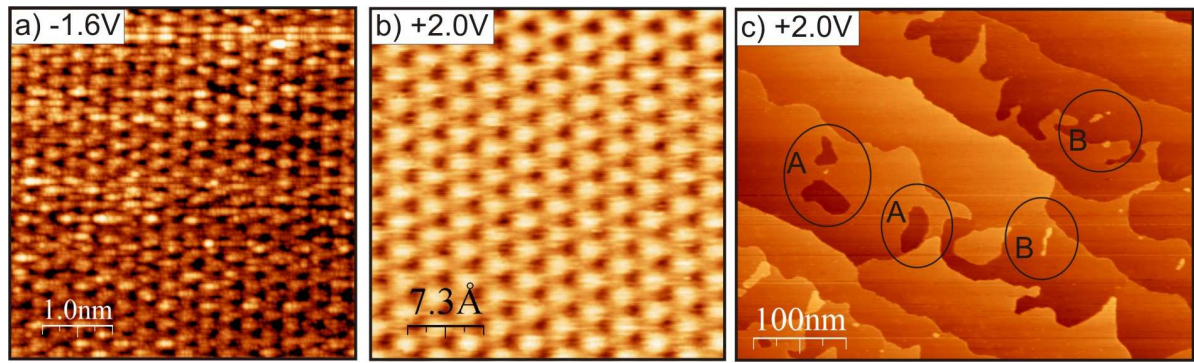


Figure 2. Scanning tunneling microscopy of Si(111):GaSe with negative (a) and positive sample bias (b). Both images show the periodicity of the GaSe-half-sheet and no defects could be localized. In c) a large scale image of a low miscut sample ($< 1^\circ$) is presented. The terrace-width is in the order of 100nm and the step height is a double Si-bilayer.

Scanning tunneling microscopy (STM) images are shown in Figure 2. On the atomic scale (Figure 2(a) and (b)), a hexagonal close-packed 1×1 structure is observed with positive and negative sample bias (see also [15]). Low energy electron diffraction also shows a 1×1 pattern with a threefold symmetry [12, 13], expected for a single domain surface termination. Wide scan STM images show a terrace structure resulting from the mis-orientation of the wafer surface with only very few defects.

Surfaces with a low miscut angle ($< 1^\circ$) exhibit large terraces widths of more than 100 nm with small holes (marked with "A" in Figure 2) and some small islands (marked with "B"). As reported in [14] and [15], the bottom of the holes is the same height as the adjacent lower terrace. Likewise, the small islands have the same height as the adjacent higher terrace. We attributed these features to the two main reorganization processes, which occur during the GaSe half-sheet formation [13]. First the gallium is moved from the T_4 -site in the $\sqrt{3} \times \sqrt{3}$ R30°-Ga (1/3 ML) to a substitutional site in the $6.3\sqrt{3} \times 6.3\sqrt{3}$ R30°-Ga (1ML) reconstructions. Therefore one monolayer of silicon must be carried away. In the second stage the gallium-reconstruction is removed stepwise by the GaSe half-sheet. The gallium is located in a top position in the GaSe-half-sheet and therefore one monolayer of silicon must be transferred to step-edges. If the diffusion-length is comparable to the size of the terrace-width (100 nm) the number of depressions and small island is very low and in the order of 10^{10}cm^{-2} as shown in Figure 2. Larger terraces lead to an increased density of these two features as earlier presented by Ueno *et al* [14] and Ohta *et al* [15]. The displaced atoms also attach at the step edges, making them more meandering than the straight edges typical of the initial substrate. Additional line and point defects related to orientational domain boundaries and substitutional defects have also been reported [15].

High-resolution Si $2p$, Ga $3d$ and Se $3d$ core-level spectra recorded using excitation of $h\nu = 140$ eV taken from the U49/2 - PGM 2 undulator beamline at BESSY [22] are shown in Figure 3. All three core-levels show only a single chemical component at

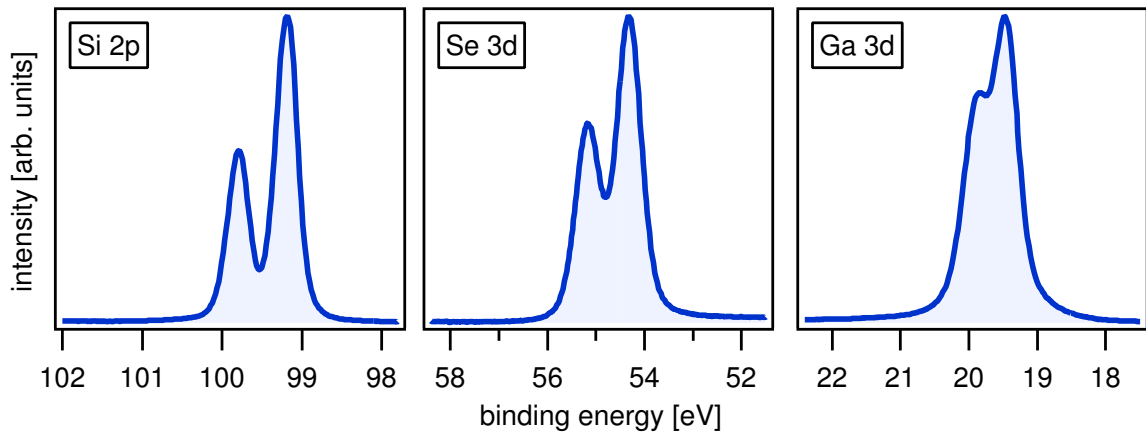


Figure 3. Si $2p$, Se $3d$ and Ga $3d$ core level spectra recorded with $h\nu = 140$ eV synchrotron radiation.

very high resolution, consistent with previous observations [7]. The core-level spin-orbit splittings of the Si $2p$, Se $3d$ and Ga $3d$ level were determined from least squares curve fitting with Voigt profiles as 0.607, 0.855 and 0.447 eV, respectively. All values being in good agreement with reported data for Si, GaAs and WSe₂ [23, 24, 25]. In contrast to other Si surfaces [18, 21, 23], the Si $2p$ core-level shows no surface core-level shift (SCLS) within our experimental resolution of 150 meV, which is determined from the Gaussian broadening of the Fermi edge emission of clean Au surface. The absence of a surface core-level shift at the Si(111):GaSe surface termination has been attributed to the non-polarity of the Si-Ga bond [7, 12]. While Ga-covered Si(111) surfaces clearly show a 300 meV SCLS due to a polar Si-Ga bond [12, 13, 26], the polarity of the bond is most likely removed by the strong attraction of electrons of the outermost Se atoms [12].

4. Scanning Tunneling Spectroscopy

To verify the absence of electronic states at the surface with energies inside the Si band gap, and to determine the surface band gap, the Si(111):GaSe surface has also been investigated by scanning tunneling spectroscopy (STS). Scanning probe images clearly confirm the unreconstructed 1×1 structure of the surface for positive and negative sample bias (see Figure 2). The voltage dependence of the tunneling current and its derivative are shown in Figure 4. The plotted curves are the average of 10 single STS-measurements. Measurement points included in the average have neither nearby substitutional defects, defects at the measuring points in the next STM-image, nor vibrations visible in the IV-curves. Our electronic noise level was ≈ 1 pA.

Taking the edges of the surface bands to be the point where the absolute value of the current drops below our 1 pA noise level, we identify the surface band gap for a GaSe bilayer on an n-type Si substrate to be 2.08 eV (Figure 4a). A similar value is

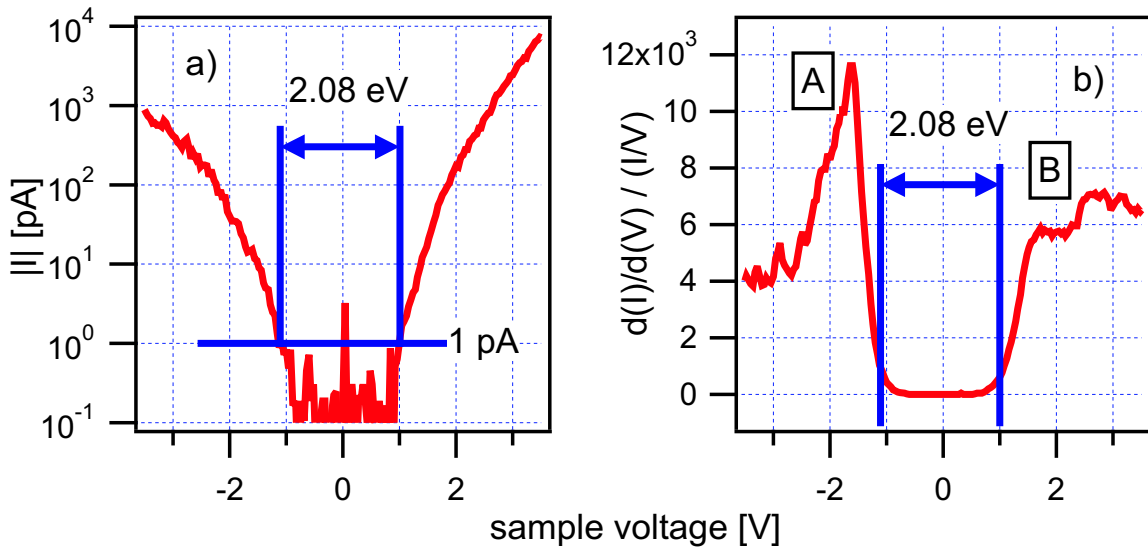


Figure 4. Scanning tunneling spectroscopy of a GaSe half-sheet on n-type silicon: a) absolute value of the current as a function of tip-sample voltage, and b) $\frac{d(I)/d(V)}{(I/V)}$, which is proportional to the density of states. The indicated points A and B correspond to tunneling conditions resulting in best images for positive and negative voltages, respectively. A surface band-gap of 2.08 eV is determined.

also observed on p-type substrates. This value is within the range of all layered bulk GaSe polytypes (~ 2.0 eV; see Ref. [27] and references therein). It thus appears that orbital interactions giving rise to the band gap in pure layered GaSe are comparable to those for the single Ga-Se layer on Si(111):GaSe.

The normalized conductance derivative in Figure 4(b) is proportional to the density of states [28, 29, 30]. The band-gap and two important points (A and B) are marked in the right plot. The value for the band-gap is taken from the left figure. The state "A" at -1.6 V (negative voltages correspond to occupied states) is most likely due to the frontier lone-pair Se p_z -orbitals (see below and Ref. [31]). To image the GaSe half-sheet with negative bias this is the minimum voltage that must be applied (see Figure 2a and Ref. [15]). The first maximum at positive bias, labelled "B", is $\sim 1.8 - 2.0$ eV above the Fermi level. By using this voltage the best images at positive bias can be recorded (see Figure 2b). In accordance with single crystal band structures, the calculation from Camara *et al* [31] shows that the conduction band of the Si(111):GaSe surface is also mostly derived from Se s -orbitals. As noted in [15], selenium orbitals are therefore most likely responsible for both tunneling directions.

5. Band Structure Determination by Photoelectron Spectroscopy

5.1. Normal emission valence band spectra

Normal emission spectra probe the electronic structure perpendicular to the surface and the surface $\bar{\Gamma}$ point. This corresponds to the ΓL direction of the silicon Brillouin zone

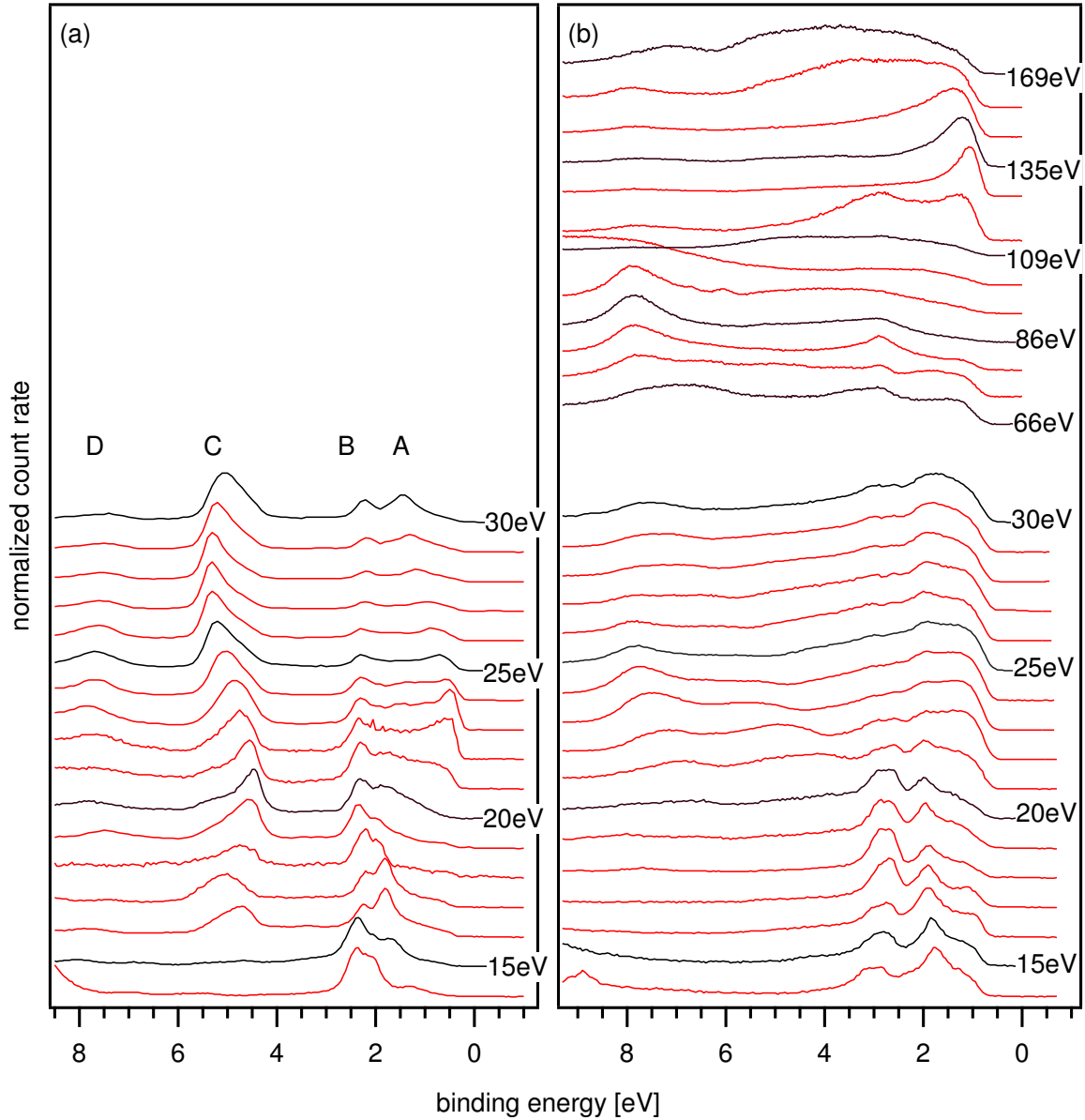


Figure 5. Normal emission valence band spectra of (a) GaSe single crystal cleaved in vacuum along the [0001] direction ($h\nu = 12 - 30$ eV) and (b) Si(111):GaSe surfaces ($h\nu = 12 - 170$ eV) at different photon energies. Binding energies are given with respect to the Fermi level as measured.

and to the ΓA direction of the hexagonal GaSe Brillouin zone. Figure 5 presents normal emission valence band spectra from a vacuum cleaved GaSe single crystal (a) and a Si(111):GaSe terminated surface (b) for a wide range of photon energies (and hence k_{\perp}).

The valence band spectra and derived band structure of the cleaved single crystal GaSe(0001) surface are in good agreement with previous studies [32, 33, 34]. The bands can be grouped into 4 different groups A to D, as indicated at the top of Figure 5(a).

In normal emission these correspond to emission from bands which are predominantly derived from Se p_z (A), Ga and Se p_x and p_y (B) and from the bonding (D) and anti-bonding (C) orbitals of the Ga-Ga bond (Ga s orbitals) [32, 33, 34, 35, 36, 37]. The band structure is well modeled by *ab initio* density functional theory [33], which closely reproduced the semi-empirical tight binding calculation of Doni *et al* [37]. As can be expected, the bands derived from the p_x - and p_y - orbitals show minimal dispersion in normal emission, while the other bands show pronounced binding energy shifts with variation of photon energy (or k_\perp).

For Si(111):GaSe, we expect the two-dimensional surface bilayer states to be independent of photon energy, with dispersing states characteristic of the underlying silicon. Features related to the Se p_x - and p_y - states (emissions indicated by (B); see Sect. 6 for assignment of spectral features) are observed at the GaSe terminated surface at similar binding energies (2.5–3.5 eV) to those for bulk GaSe (2–3 eV). The difference in binding energy is mostly due to a different Fermi level position. The emissions from the p_z -orbitals of the GaSe single crystal (A) are superimposed by Si bulk bands at the Si(111):GaSe surface (see below). Emissions in regions C and D are suppressed in intensity for the Si(111):GaSe bilayer. In bulk GaSe, these emissions are related to the Ga-Ga bonds, which at the Si(111):GaSe are replaced by Si-Ga bonds and overlap strongly with Si-Si bonding orbitals.

The observed electronic transitions (peaks and shoulders) for Si(111):GaSe are plotted versus wave vector in Figure 6, where the perpendicular component k_\perp of \mathbf{k} has been determined assuming direct transitions to free-electron final states with an inner potential of 12.5 eV. This value of the inner potential is consistent with the value of 13 ± 1 eV found when fitting low kinetic energy photoelectron diffraction data [7]. Although a free-electron final state model has also led to reasonable interpretation of data for electronically decoupled thin films of InSe [38], it is not appropriate for a full interpretation of spin-resolved normal emission valence band spectra of GaSe [34].

In contrast to the bulk GaSe data, the binding energies of most of the transitions observed for the Si(111):GaSe surface do not depend on k . Such dispersionless states are expected for surface state emissions, and are highlighted with lines in the figures. Also visible, especially in the fourth Brillouin zone, are two dispersing Si bulk states, which are indicated by dashed thick lines in Figure 6. The domination of the spectra by surface state emissions is not surprising as the GaSe half-sheet is almost as thick as the minimum of the photoelectron escape depth, which is attained at ~ 50 eV electron kinetic energy. Away from the sample normal, however, bulk states are somewhat more visible, as seen in Si(111):As [21] and Si(111):AlSe [39]

Of the five surface states observed at $\bar{\Gamma}$, only the highest (associated with the lone pair) and lowest (the Si-Ga bonding state) are strong in both the high and low photon energy data. This may be due to different orientations of the sample relative to the light polarization in the two experiments.

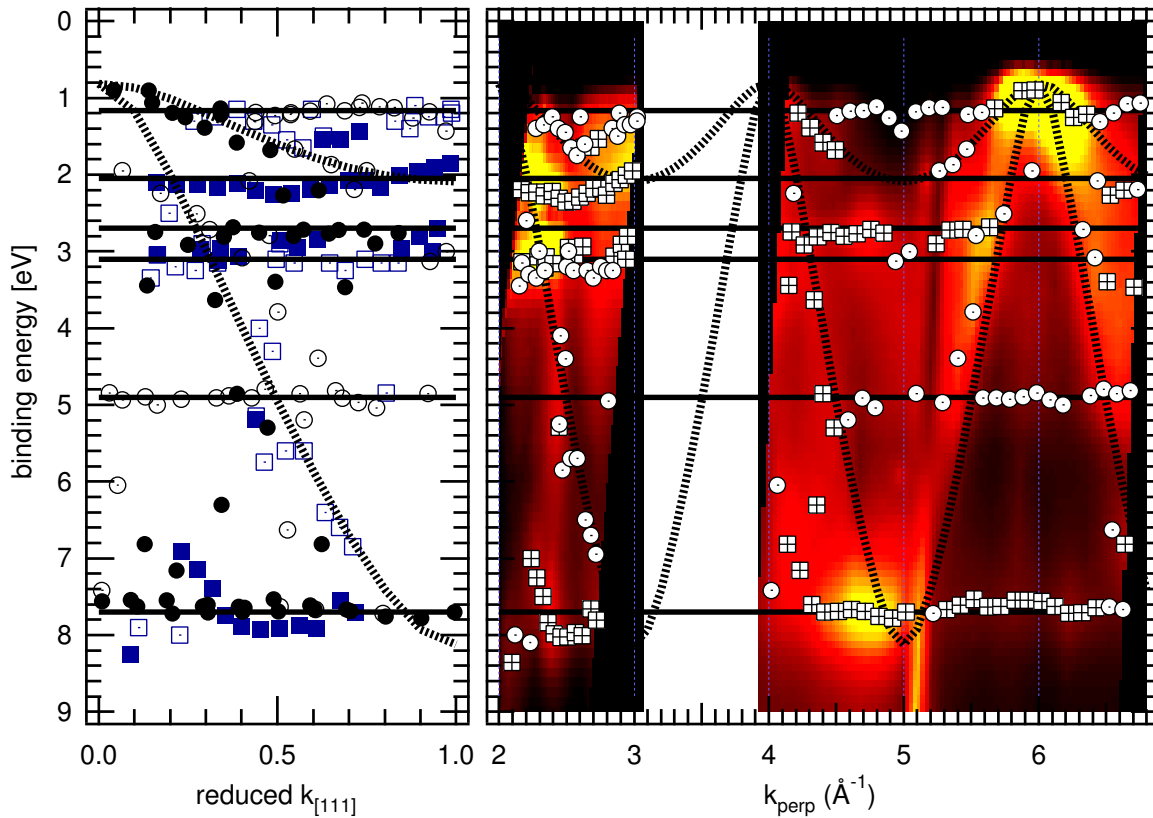


Figure 6. Binding energies of Si(111):GaSe transitions versus wave vector k_{\perp} for the spectra shown in Figure 5(b). The perpendicular component of the wave vector k_{\perp} was calculated using free electron final states and an inner potential of 12.5 eV. On the left, the data are reduced to the first Brillouin zone, while the data are plotted *vs.* the actual value of k_{\perp} on the right. Filled symbols on the left correspond to BESSY data ($h\nu = 14 - 30$ eV, $k_{\perp} \sim 2 - 3$ \AA^{-1}), open symbols to ALS data ($h\nu = 63 - 169$ eV, $k_{\perp} \sim 4 - 7$ \AA^{-1}). Squares and circles in both data sets correspond to peaks and shoulders in the data, respectively. The image on the right reflects the intensities, normalized separately for each photon energy. Silicon bulk bands along ΓL are indicated by dashed thick lines, and horizontal lines highlight non-dispersing states. The structure in the data near $k_{\perp} = 5$ reflects Si KLL Auger emission overlapping the valence band (see Figure 5, $h\nu = 102$ eV).

5.2. Angle dependent valence band spectra

Angle dependent photoelectron spectra taken with $h\nu = 21$ eV excitation energy along the ΓM direction of the hexagonal Brillouin zone for a vacuum cleaved single crystal GaSe(0001) surface and along the corresponding $\bar{\Gamma}\bar{\text{M}}$ direction of the surface Brillouin zone of the Si(111):GaSe terminated surface are presented in Figure 7. Spectra taken along the ΓK direction of the same samples are given in Figure 8.

The single crystal spectra show a large number of intense emissions corresponding to the number of atoms in the unit cell (8). Large binding energy shifts along both crystallographic directions are evident. The energy dispersion agrees with those given

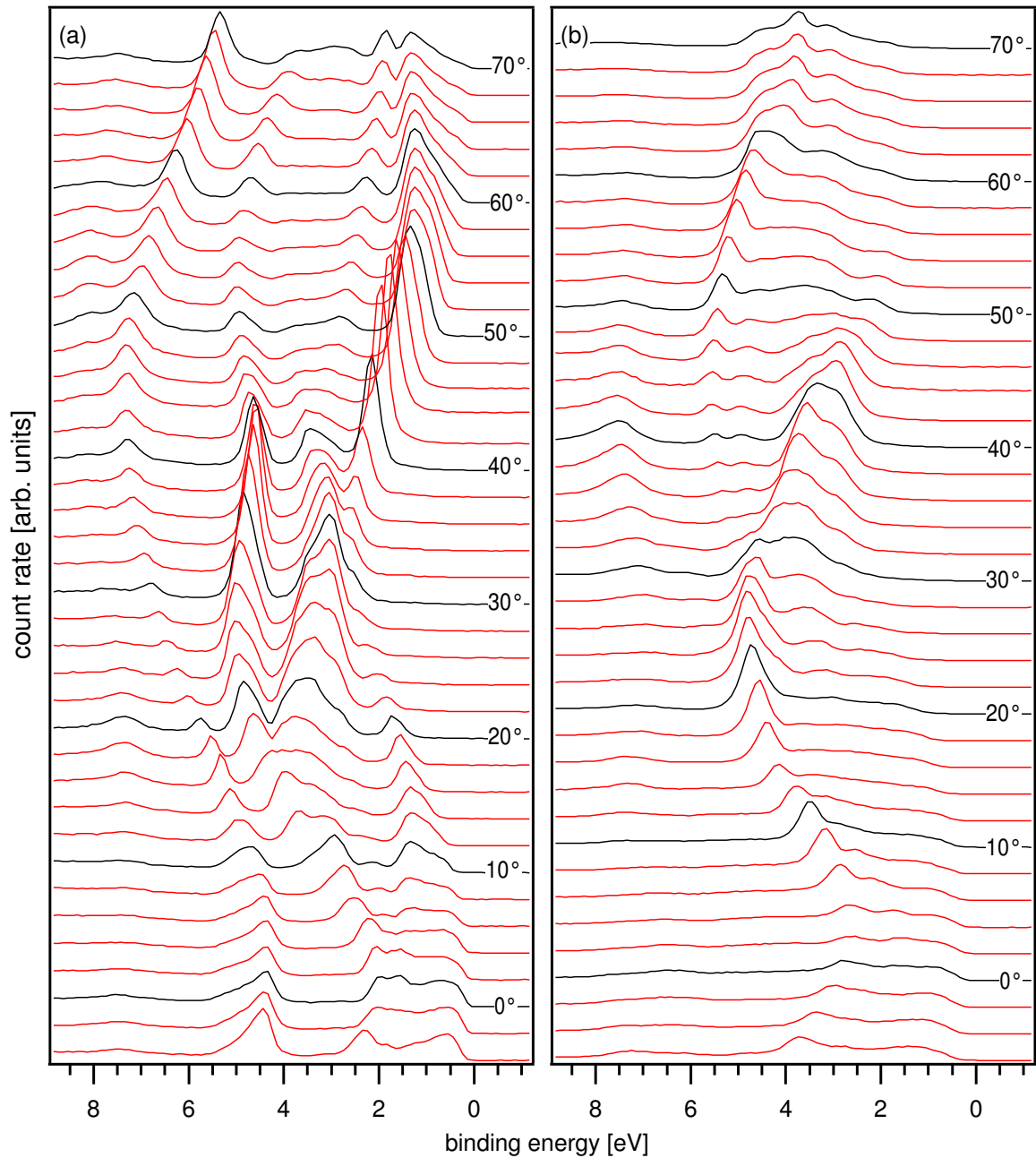


Figure 7. Emission angle dependence of valence band spectra recorded with linearly polarized photons with $h\nu = 21$ eV energy at BESSY for a GaSe single crystal (a) and the Si(111):GaSe surface termination (b). The spectra were taken along the ΓM direction of the hexagonal Brillouin zone.

in the literature by Thiry *et al* [32] and Plucinski *et al* [33]. The emissions with lowest binding energy are observed at 0° emission angle, indicating a valence band maximum at Γ in agreement with the literature [32, 33, 35, 37, 40]. The spectra taken from the Si(111):GaSe surface termination also show pronounced structures with strongly dispersing transitions for both symmetry directions. As expected from the

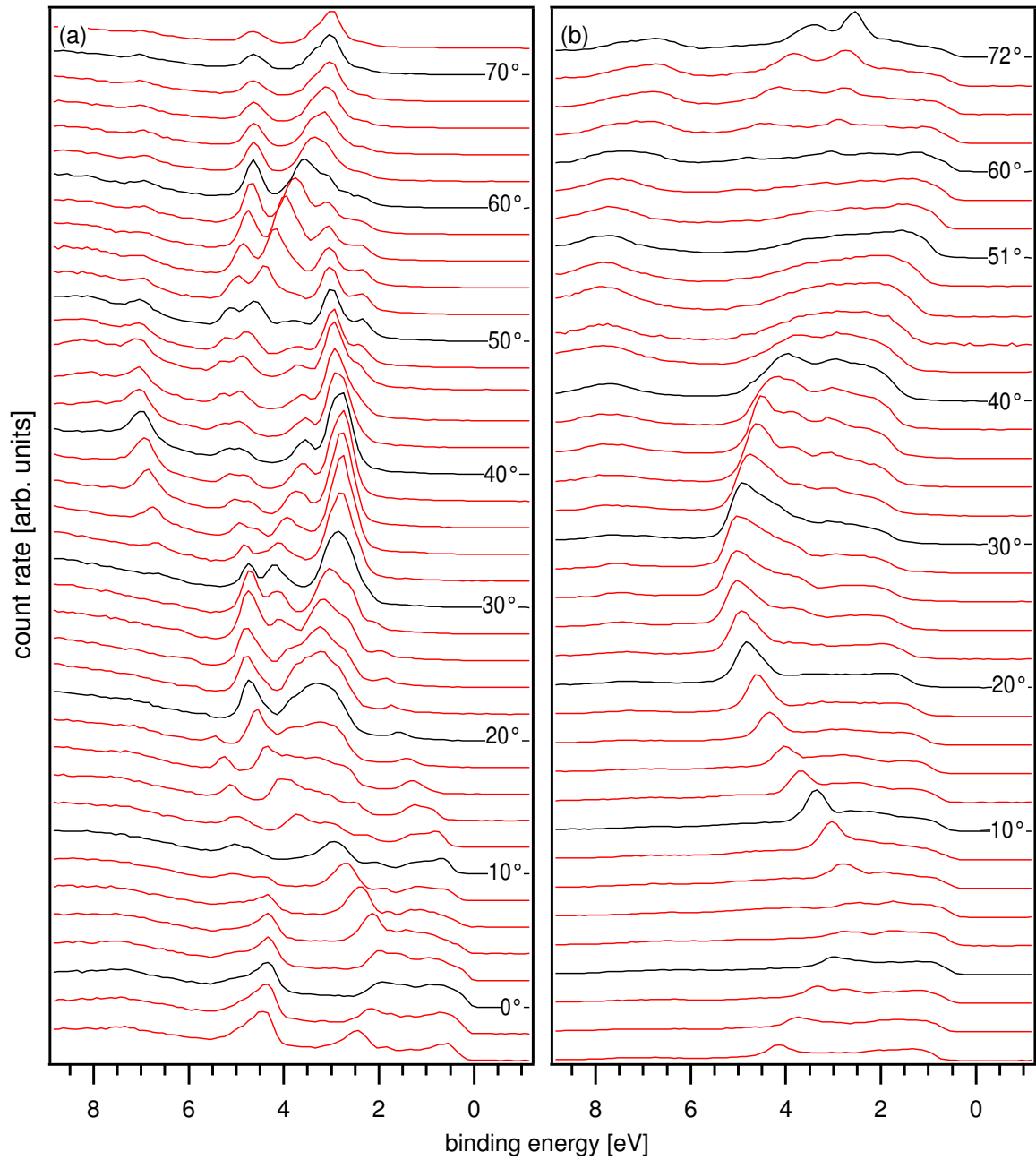


Figure 8. Emission angle dependence of valence band spectra recorded with linearly polarized photons with $h\nu = 21$ eV energy at BESSY for a GaSe single crystal (a) and the Si(111):GaSe surface termination (b). The spectra were taken along the ΓK direction of the hexagonal Brillouin zone. The polarization vector lies in the plane containing both ΓK and the emitted electron.

crystallographic structure of an ideal surface termination, they are noticeably different for the two directions, indicating a well prepared surface termination layer.

On first glance at Figures 7 and 8, spectra taken from the GaSe-terminated Si(111) surface show little resemblance to the single crystal data. However, the dissimilarity is

mostly caused by different intensities of the various emissions. This is seen clearly in Figure 9, which shows the energy dispersions along ΓM and ΓK (determined from the spectra given in Figures 7 and 8) for the GaSe single crystal and along $\bar{\Gamma}\bar{\text{M}}$ and $\bar{\Gamma}\bar{\text{K}}$ for the Si(111):GaSe surface. Binding energies derived from similar data sets taken with He I ($h\nu = 21.2$ eV) excitation and with synchrotron radiation ($h\nu = 72, 90$ eV) from Si(111):GaSe are also included; they were taken in Seattle (He I) and at the Advanced Light Source, respectively. The He I photons are unpolarized; the polarization vector for the ALS data is perpendicular to the plane containing ΓM ; the polarization direction for the BESSY data is in the plane containing ΓM and the emitted electron wave vector.

Several bands can be identified that show almost identical energy dispersions for both surfaces. Simple sinusoidal bands have been fitted to the bands of the Si(111):GaSe surface termination that are common to the different photon energies (hence associated with the surface). These same curves are superimposed on the band structure of the GaSe single crystal for a better comparison. The similarity between the band structures of bulk GaSe and the van der Waals-terminated Si(111):GaSe surface are obvious for the ΓM direction; the similarity is less pronounced for the ΓK -direction.

6. Electronic Structure of the Surface

6.1. Phenomenological Model of Electronic States

The striking similarity between the electronic bands for the Si(111):GaSe surface and those for the cleaved GaSe single crystal surface leads us to describe the bands starting from the electronic structure of bulk GaSe. In this section we outline a phenomenological description of the electronic states at the Si(111):GaSe surface based on consideration of molecular orbital contributions to the electronic structure of bulk GaSe. An analogous approach has recently been used to discuss inter-layer interactions in layered metal dichalcogenides [41, 42]. In the following section, we discuss the bands in terms of the isoelectronic Si(111):H, Si(111):As and Si(111):AlSe and the connections between passivated Si(111) and layered GaSe.

A detailed description of the electronic structure of III-VI-compounds is given in the literature [33, 35, 37, 40]. GaSe is a direct gap semiconductor with a valence band maximum and a conduction band minimum located at Γ for the β (2H) polytype, or at Z for the γ (3R) polytype, respectively. The difference in electronic structures of the various polytypes is mainly explained by the different extension of the unit cell along c . Since we are only dealing with a half-sheet of a single layer, the distinction between different polytypes is not important here (see Figure 1). Energy bands for bulk β -GaSe (2H polytype), as calculated by Doni *et al* using a semiempirical tight binding approach [37], are reproduced in Figure 10(a). These band structures quite well reproduce the experimental band structures of GaSe and InSe (see also Ref. [38]) and are very close to state-of-the-art density functional theory calculations [33].

In the simplest description of the electronic structure of layered III-VI compounds,

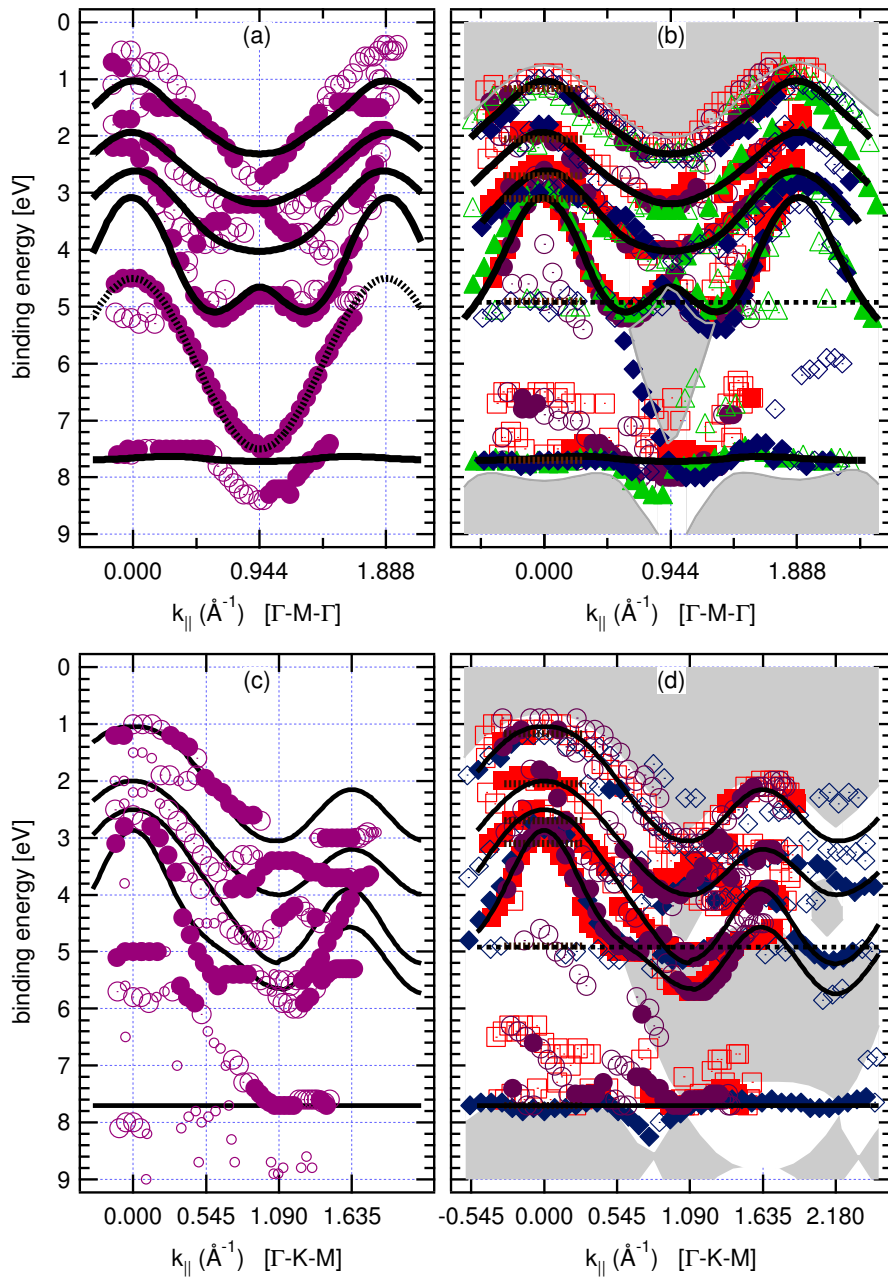


Figure 9. Electronic structure along Γ M of (a) a GaSe single crystal and (b) Si(111):GaSe. The band structures are determined from angle-resolved valence band spectra (see Figure 7) taken with 21 (\circ), He I (\square) 72 (\diamond) and 90 eV (\triangle), respectively. Filled symbols correspond to pronounced peaks, open symbols to shoulders and weaker structure. The shaded areas in (b) represent surface projected Si bulk bands. Solid lines in (a) and (b) are sinusoidal curves fitted to the data points of the single crystal bands. The bands shown in (c) and (d) for the Γ K-direction are for single crystal GaSe and Si(111):GaSe, respectively. The meaning of the symbols is the same as in (a) and (b).

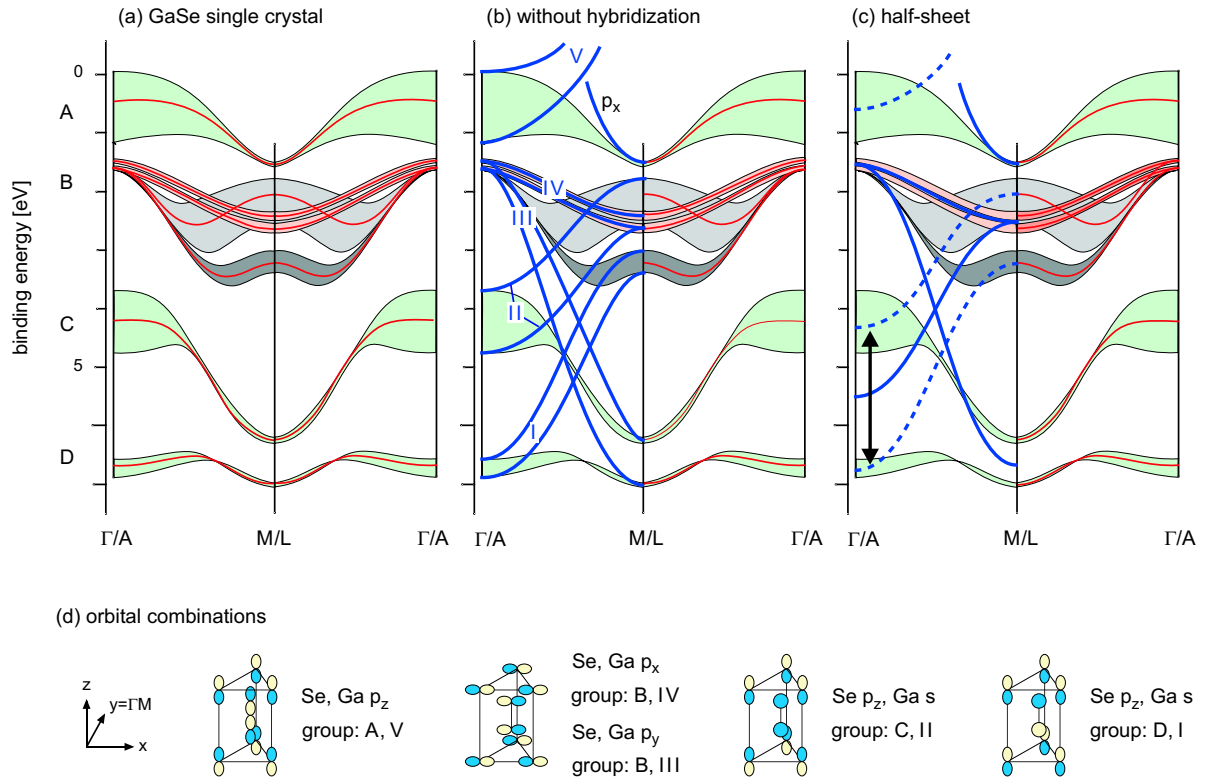


Figure 10. Semiempirical tight binding band structure of GaSe along ΓM according to Doni *et al* (a) [37]. Upper and lower limits of the color-shaded areas correspond to energy bands in the central ΓM plane of the hexagonal Brillouin zone and indicate inter-layer splitting and red lines approximately halfway between the upper and lower limits to dispersion in the top plane of the Brillouin zone (along AH). Lines given in (b) indicate the dispersion of energy bands in the *hypothetical* absence of hybridization. Corresponding lines in (c) are tentative non-hybridized energy dispersions for a *hypothetical* isolated Ga-Se half-sheet. The bonding/antibonding splitting of the Ga-Ga bond is indicated by the arrows and should not occur for an *isolated* half-sheet.

the valence band maximum is derived from chalcogen p_z -orbitals and the conduction band minimum from metal p_z -orbitals (symmetrized combinations of molecular orbitals are given by Doni *et al* [37] and are shown in Figure 10(d)). In the real electronic structure, hybridization between chalcogen and metal states is important. A more detailed analysis of the contributions to the band edge states for the isostructural and isoelectronic compound InSe is given by Gomes da Costa *et al* [40], revealing a valence band maximum composed of 70% Se p_z and 30% In p_z -orbitals, while the conduction band minimum is composed of Se s (37.5%), Se p_z (25%) and In s -orbitals (37.5%).

As a result of hybridization, the bands derived from given symmetrized orbital combinations do not directly correspond to calculated energy bands. In terms of energy band structure, bands may only cross without interaction (hybridization) if they have different symmetry, while hybridization of energy bands leads to an energy gap. Using symmetrized combinations of atomic orbitals [37], *hypothetical* energy bands *without hybridization* can be outlined for bulk GaSe. The result is shown in Figure 10(b). The

construction of non-hybridized energy bands is easily accomplished for the ΓM direction, which corresponds to the crystallographic y -axis as shown in Figure 10(d).⁺ The given *hypothetical* energy bands for the different symmetrized orbital combinations, shown in Figure 10(d), exhibit the dispersions expected from simple tight binding considerations [43, 44]. The bands derived from s - and p_z -orbitals (labeled I, II, and V in Figure 10(b)) disperse upwards with increasing k_{\parallel} , while those derived from p_x - and p_y -orbitals (labeled III and IV in Figure 10) disperse downwards. Binding energies for the various orbital combinations at Γ and M are taken from Doni *et al* [37].

Of interest for the Si(111):GaSe surface are those electronic states expected to persist for an isolated half-sheet layer. These can, at least partly, be identified *a priori*. First of all, *inter*-layer interactions, which are indicated in Figure 10 by the shaded grouping of bands (perpendicular dispersion), have to be omitted (see also description of electronic states in Reference [41]). As a consequence, the pairs of *hypothetical, non-hybridized* bands indicated by roman numerals I, II, and V in Figure 10(b) have to be replaced by a single band located approximately in the center of the shaded regions at the boundaries of the Brillouin zone. The bands derived from p_x - and p_y -states (groups III and IV) have a negligible inter-layer splitting and are therefore not significantly affected.

In addition, splitting the layer in half between the two Ga atoms will strongly modify some *intra*-layer interactions. Cutting the layer between the Ga planes has the strongest impact on states derived from p_z and s orbitals, as these have a large overlap along the c -direction, and a weaker impact on the p_x and p_y (Ga-Se bonding) states. Since the Se atomic layers are well separated (4.78 Å), the main consequence of splitting the layer in half is removal of the Ga-Ga interaction. The bonding and anti-bonding combinations with predominant Ga 4s character are given by bands I and II (see Figure 10). An *isolated* half-sheet of GaSe should have a single band, instead of the two bands I and II, as the Ga-Ga bond is removed. Hybridization of the chalcogen p_x and p_y -states with the Ga p_x and p_y -states (bands labeled III and IV in Figure 10) is not strongly modified since the Ga-Se bond length and geometry is nearly unchanged. The (small) splitting between the intralayer bonding (labeled as x^+ in Ref. [41], Figure 2) and anti-bonding (x^-)-states is removed, while maintaining a similar dispersion along ΓM .

Using the above arguments, tentative energy bands for a *hypothetical, isolated* GaSe half-sheet layer are drawn in Figure 10(c). The p_x and p_y -bands (bands III and IV) are modified only by the missing inter-layer interactions. The former Ga-Ga bonding and antibonding states (groups I and II) are represented by dashed lines in Figure 10(c). The splitting between them should be absent for an isolated half-sheet (with no Ga-Ga bonds); the two bands are replaced by a single band approximately half-way between the dashed bands, indicated in Figure 10(c) by a solid line dispersing upwards along ΓM . However, at the Si(111):GaSe surface, the Ga-Ga bond is replaced by a Si-Ga

⁺ The procedure is less straightforward for the ΓK direction, as the ΓKHA -plane of the hexagonal Brillouin zone is not a mirror plane, in contrast to the ΓMLA -plane (see also discussion of selection rules for dipole transitions in Ref. [41])

bond. Although the dispersion of the corresponding bonding and anti-bonding states will in principle be similar to those of the Ga-Ga bond, the energies and band widths of the states belonging to the Si-Ga bond are not known. One might expect noticeable differences between the asymmetric Si-Ga bond and the non-polar Ga-Ga bond in GaSe.

Finally, we note the experimentally observed energy bands should follow the dispersion of hybridized bands and not those of the outlined hypothetical non-hybridized bands. Rather, construction of non-hybridized bands enables identification of those parts of the GaSe band structure expected to persist in the half-sheet layer.

6.2. Comparison with Experiment

We start with the band we expect to be the least perturbed between the bulk and half-layer GaSe, namely the p_x - and p_y -states of the Ga-Se bilayer. The emission at a binding energy of $BE \approx 3$ eV at $\bar{\Gamma}$ (see Figures 7(b) and 8(b)) can be attributed to these states (band III and IV in bulk GaSe). The p_y -states (band III) strongly disperse downwards and give rise to strong emissions at $BE \approx 8$ eV at the M point of the Brillouin zone (see Figure 7(b) at 40° emission angle). The downward dispersion of the p_x -states is much weaker since they are oriented perpendicular to the $\bar{\Gamma}\bar{M}$ direction. They are expected to show up at $BE \approx 4$ eV at the \bar{M} point. Similar binding energies are expected at \bar{M} from the upward dispersing Si-Ga bonding and anti-bonding states (bands I and II), from which they can not be distinguished. However, it can be expected, that the p_x -states contribute to the number of intense emissions near \bar{M} at this energy.

Interestingly, the Si(111):GaSe surface shows emissions at Γ at binding energies close to those of the single crystal Ga-Ga bonding and antibonding states. This is evident from the general agreement between both band structures (Figure 9). These emissions are most likely attributed to states from the Si-Ga bond, implying that the binding energies of the bonding and antibonding Si-Ga states of Si(111):GaSe are very close to those of the Ga-Ga states in GaSe single crystals. This evidence for non-polarity in the Si-Ga bond is consistent with the absence of a Si surface core-level shift in high-resolution Si $2p$ core-level spectra (see Refs. [7, 12] and Figure 3) and the observation of flatband conditions at the surface [12]. As discussed in Ref. [12], a Si-Ga bond is generally polar due to the larger electronegativity of Si compared to Ga (Pauling electronegativity = 1.90 and 1.81, respectively), but the interface Si-Ga bond in Si(111):GaSe becomes non-polar as a result of the Ga-Se bonds. The large electronegativity of Se (Pauling electronegativity = 2.55) leads to charge transfer from Ga to Se and reduces the ability of Ga to donate electrons to the silicon, effectively increasing its electronegativity to essentially equal that of Si.

The top of the GaSe valence band (transitions with lowest binding energies) has Γ_4^- symmetry in GaSe single crystals [37, 38, 41], and is primarily derived from the Se lone-pair p_z states. The corresponding lone-pair emissions are also clearly observed at the Si(111):GaSe surface, absent the splitting associated with inter-layer interactions. The upward dispersion with increasing k_{\parallel} , expected for non-hybridized p_z -states (Figure

10(c)), is not observed, which is a consequence of the hybridization between p_z - and p_x , p_y -states (see section 6.1). It is also not expected that the hybridization of these states is absent at the surface, as it has a lower symmetry than the corresponding GaSe single layer (missing horizontal reflection plane). The similar hybridization of the layer compared to bulk states has the important consequence of producing a surface without electronic states within the Si band gap, leading to an electronically passivated surface [12].

A noticeable difference between the band structures of GaSe and the Si(111):GaSe surface termination is the bulk band dispersing downwards from $BE \approx 5$ eV at $\bar{\Gamma}$ to $BE \approx 8$ eV at \bar{M} or \bar{K} . The corresponding states of the Si(111):GaSe give rise to weak emissions close to $\bar{\Gamma}$, which are not observed at higher emission angle (see Figures 7, 8, and 9). A downward dispersing band is detected in the 72 eV spectra, which, however, is more likely due to emission from a Si bulk band. For the GaSe single crystal, this band is mainly composed of Ga s and Se p_z orbitals at Γ and of Se p_y orbitals at \bar{M} (see Figure 10 and Ref. [37]). Due to hybridization of the bands along $\Gamma\bar{M}$ (Σ -direction), the band is a mixture of both constituents. Along Σ in the GaSe bulk, hybridization between p_z and p_y orbitals is possible since both transform identically under the symmetry operations of the point group Σ , which are the identity, a two-fold rotation along y (C_2), and reflections at the xy - (σ_h) and yz -planes (σ_v), respectively [41]. In the surface layer, however, neither C_2 nor σ_h are symmetry operations. Due to the lower symmetry, it is expected that hybridization between the different orbitals is still possible. The same holds for the corresponding direction in bulk Si ([112]), which only has σ_v as higher symmetry element. It is thus expected that the p_y and p_z can still hybridize as also observed for the outermost Se atoms (see preceding paragraph). The apparent absence of the band at the Si(111):GaSe surface is therefore attributed to a low photoemission intensity.

6.3. Electronic States of Passivated Si(111)

An alternate approach to the Si(111):GaSe surface from that of the basic building block of bulk GaSe is to consider it as an ideal termination of bulk silicon. As mentioned above, the Si(111):GaSe surface is isoelectronic to the well-studied Si(111):H and Si(111):As passivated surfaces (see Figure 1), consisting of bulk silicon plus either (Si-Si-H), (Si-As) or (Ga-Se). All three terminations contribute 9 valence electrons that may give rise to states separate from those of bulk Si. We can separate these into the 2 electrons in an orbital near the surface (the Si-H bond, the As lone-pair or the Se lone-pair, respectively), the 6 electrons in the surface bilayer bonds (Si-Si, Si-As or Ga-Se), and the electron contributed to the bond between the bilayer and the substrate (Si-Si, Si-Si or Si-Ga). We thus expect 5 fully occupied states near the surface for these 9 electrons plus one electron from the silicon atom beneath, which bonds to this surface layer. Indeed, the normal emission data at variable photon energy for Si(111):GaSe (Figures 5 and 6), in addition to the two bulk Si states dispersing from Γ to L, show five states

that do not disperse with photon energy (Figure 6), but do exhibit dispersion parallel to the surface with the symmetry of the surface Brillouin zone (Figure 9). An additional weak shoulder at a binding energy around 5 eV in Figure 6 appears only at high photon energy (above the Si L-edge) and may be an inelastic loss feature or defect state, as it also does not disperse with k_{\parallel} . Given the strong feature (C) in bulk GaSe near this energy associated with the Ga-Ga bond, a candidate defect state is a Ga_{Si} substitutional defect, leading to a Ga-Ga bond. These defects are the most common seen with STM [15].

We consider first the electrons physically closest to the surface, in s - p_z orbitals of either the Si-H bond, the As lone-pair or the Se-lone pair. Comparison of these systems is simplest at the \bar{K} -point, where the bulk Si bands have the largest gaps. Near the zone center, the lone-pair state largely overlaps the silicon valence band maximum and is difficult to distinguish. The energy of this state at the \bar{K} -point relative to E_{VBM} is a sensitive measure of the interface dipole between the underlying bulk Si and the surface [45]. At \bar{K} , this state for Si(111):H has binding energy 4.8 eV below the Si valence band maximum (E_{VBM}) [19], lying in an empty pocket of the projected bulk Si bands. For Si(111):As, the lone pair state at \bar{K} is 1.8 eV below E_{VBM} [21], or about 0.5 eV above the highest Si band at \bar{K} . The equivalent state for Si(111):GaSe lies right at the edge of the projected bulk Si bands, at an energy about 2.3 eV below E_{VBM} . The equivalent state for Si(111):AlSe has a similar energy to that for Si(111):GaSe [39].

The difference in the surface dipole between a Si-As bilayer and a Ga-Se bilayer can be thought of as moving a layer of protons up towards the surface, turning Si^{4+} into Ga^{3+} and As^{5+} into Se^{6+} , which should decrease the electrostatic potential energy of an electron on the surface. The equivalent operation shifting a layer of protons in next bilayer down, comparing a buried Si-Si bilayer to a buried Ga-As bilayer (*i.e.*, $Si - Si \equiv Si - Si \equiv As$ vs. $Si - Ga \equiv As - Si \equiv As$), has been calculated to cause a -0.4 eV difference in the lone-pair energy at \bar{K} [45], consistent with the -0.5 eV difference we observe between Si(111):As and Si(111):GaSe. Si(111):H, on the other hand, may be generated in a thought experiment by moving a layer of protons from Si(111):As outward to the other side of the state in question ($Si - Si \equiv Si - Si \equiv As$ vs. $Si - Si \equiv Si - Si \equiv Si - H$), for a smaller electrostatic shift, but in the same direction, as for Si(111):GaSe. The much lower energy of the state for Si(111):H is attributed to the large bonding interaction between the Si and H orbitals. The surface Si bilayer is essentially a bulk environment, and the Si-H bond is close in polarity and energy to that of the Si-Si bond.

We next discuss the "back-bond" states in the surface bilayer, which we associate with the states of binding energy $\sim 2 - 3$ eV at $\bar{\Gamma}$ that disperse downwards towards \bar{M} and \bar{K} . For Si(111):As, the only difference between the predicted bulk Si transitions and the observed surface band structure for states in this energy range is a small deviation near the pockets in the projected bulk band structure near \bar{M} and \bar{K} [21]. This has been attributed to the breaking of symmetry along the Si-As bond relative to the bulk Si-Si bond pulling the states into the bulk gap. Some surface resonances are found in this

energy region for Si(111):H, mainly near the \bar{K} point, but there is no clear deviation from bulk energies and dispersions. For Si(111):GaSe, on the other hand, the "back-bond" states show a much larger resemblance to those of bulk GaSe (discussed above) than bulk Si, which is to be expected due to the very different polarity of the bonds and energies of the atomic states contributing to them.

Finally, the states bonding the surface layer to the substrate might be expected to be barely changed from bulk Si for Si(111):H and Si(111):As, and somewhat modified for Si(111):GaSe. Indeed, all three surfaces show a weakly dispersing state at a binding energy around 8 eV that may be associated with this bond.

7. Summary and Conclusions

The electronic structure of the Si(111):GaSe van der Waals surface termination has been studied by photoelectron spectroscopy and scanning tunneling spectroscopy. A surface band gap of 2.1 eV is detected, which is very close to the bulk GaSe band gap. The large surface band gap, which is approximately symmetric with respect to the Si bulk gap, is the origin for the good electronic passivation of this surface. A large number of electronic bands is determined at the surface. Their dispersion with emission angle is similar to those of bulk GaSe bands, which have been measured for comparison. The electronic structure of the Si(111):GaSe surface has consequently been discussed in terms of a molecular orbital description of the GaSe bulk band structure, taking hybridization effects into account. This procedure is justified for two main reasons. First, the arrangement of the Ga and Se atoms at the surface are almost identical to those of a half-sheet of crystalline GaSe and the topmost silicon atoms also occupy nearly ideal Si lattice sites. The second reason is the non-polarity of the Si-Ga bond, which is introduced by the polar Ga-Se bond, leading to an effective electronegativity of Ga close to those of Si. The non-polarity of the Si-Ga bond at the surface is evident from the absence of a surface core-level shift of the Si 2*p* level and from the binding energies of the valence states attributed to the Si-Ga bond, which is very close to those of the Ga-Ga bond states in bulk GaSe. The states may also be interpreted in terms of a passivated termination of bulk silicon, and were compared with Si(111):H and Si(111):As to identify the states in terms of the surface bonding and lone-pair levels.

Acknowledgments

Productive discussions and experimental support with Fumio S. Ohuchi, Eli Rotenberg and Shuang Meng, experimental support by J. Lehmann and the staff at BESSY and ALS as well as financial support from German DFG and BMBF as well as US NSF (DMR-0102427 and DMR-9801302) are gratefully acknowledged. MO acknowledges support from the Alexander von Humboldt Foundation during her sabbatical in Darmstadt. Experiments were performed at the Advanced Light Source of Lawrence Berkeley National Laboratory operated by the U.S. DOE under Contract No. DE-AC03-

76SF00098.

References

- [1] Koma A, Sunouchi K and Miyajima T 1985 *J. Vac. Sci. Technol. B* **3** 724
- [2] Jaegermann W, Klein A and Pettenkofer C 2000 in *Electron Spectroscopies Applied to Low-Dimensional Materials* edited by Hughes H I and Starnberg H P (Dordrecht: Kluwer Academic Publisher)
- [3] Liu K Y, Ueno K, Fujikawa Y, Saiki K and Koma A 1993 *Jpn. J. Appl. Phys.* **32** L434
- [4] Jedrecy N, Pinchaux R and Eddrief M 1997 *Phys. Rev. B* **56** 9583
- [5] Koebel A, Zheng Y, Pétrouff J F, Boulliard J C, Capelle B and Eddrief M 1997 *Phys. Rev. B* **56** 12296
- [6] Meng S, Schroeder B R and Olmstead M A 2000 *Phys. Rev. B* **61** 7215
- [7] Meng S, Schroeder B R, Bostwick A, Olmstead M A, Rotenberg E and Ohuchi F S 2001 *Phys. Rev. B* **64** 235314
- [8] Amokrane A, Sébenne C A, Cricenti A, Ottaviani C, Proix F and Eddrief M 1998 *Appl. Surf. Sci.* **123/124** 619-625
- [9] R. Rudolph, C. Pettenkofer, A. Klein and W. Jaegermann, *Appl. Surf. Sci.* **167**, 122 (2000).
- [10] Jaegermann W, Rudolph R, Klein A and Pettenkofer C 2000 *Thin Solid Films* **380** 276-281
- [11] Rudolph R, Pettenkofer C, Klein A and Jaegermann W 2000 *Appl. Surf. Sci.* **167** 122-124
- [12] Fritsche R, Wisotzki E, Islam A B M O, Thissen A, Klein A, Jaegermann W, Rudolph R, Tonti D and Pettenkofer C 2002 *Appl. Phys. Lett.* **80** 1388-1390
- [13] Fritsche R, Wisotzki E, Thissen A, Islam A B M O, Klein A, Jaegermann W, Rudolph R, Tonti D and Pettenkofer C 2002 *Surf. Sci.* **515** 296-304
- [14] Ueno K, Shirota H, Kawamura T, Shimada T, Saiki K and Koma A 2002 *Appl. Surf. Sci.* **190** 485-490
- [15] Ohta T, Klust A, Adams J A, Yu Q, Olmstead M A and Ohuchi F S 2004 *Phys. Rev. B* **69** 125322
- [16] Meng S 2000 Ph.D. Dissertation, University of Washington.
- [17] Pashley M D 1989 *Phys. Rev. B* **40** 10481
- [18] Hricovini K, Gunther R, Thiry P, Taleb-Ibrahimi A, Indlekofer G, Bonnet J E, Dumas P, Petroff Y, Blase X, Zhu X, Louie S.G, Chabal Y J and Thiry P A 1993 *Phys. Rev. Lett.* **70** 1992
- [19] Gallego S, Avila J, Martin M, Blase X, Taleb A, Duma, P and Asensio M C 2000 *Phys. Rev. B* **61** 12628
- [20] Olmstead M A, Bringans R D, Uhrberg R I G and Bachrach R Z 1986 *Phys. Rev. B* **34** 6401
- [21] Uhrberg R I G, Bringans R D, Olmstead M A, Bachrach R Z and Northrup J E *Phys. Rev. B* **35** 3945
- [22] Batchelor D R, Follath R and Schmeisser D 2001 *Nucl. Instr. and Meth. A* **467-468** 470-473
- [23] Paggel J J, Theis W, Horn K, Jung C, Hellwig C and Petersen H 1994 *Phys. Rev. B* **50** 18686-18689
- [24] McLean A B 1989 *Surface Science* **220** L671-L678
- [25] Klein A 1994 *it Photoelektronenspektroskopie an Schichthalbleiter/Metall Grenzfläen* (Konstanz: Hartung-Gorre Verlag)
- [26] Bringans R D, Olmstead M A, Uhrberg R I G, Bachrach R Z 1987 *Appl. Phys. Lett.* **51** 523
- [27] Bucher E 1992 in Aruchamy A (Ed) *Photoelectrochemistry and Photovoltaics of Layered Semiconductors* (Dordrecht: Kluwer Academic Publishers) 1-81
- [28] Tersoff J and Hamann D R 1985 *Phys. Rev. B* **31** 805-813
- [29] Endo K, Arima K, Kataoka T, Hirose K, Oshikane Y, Inoue H, Kuramochi H, Sato T and Mori Y 1998 *Appl. Phys. A* **66** 145-148
- [30] Kenji M 1994 *Jpn. J. Appl. Phys.* **34** 3657-3661
- [31] Camara M O D, Mauger A and Devos I 2002 *Phys. Rev. B* **65** 125206; *ibid.* 205308
- [32] Thiry P, Petroff Y, Pinchaux R, Guillot C, Ballu Y, Lecante J, Paigné J and Levy F 1977 *Solid St. Commun.* **22** 685

- [33] Plucinski L, Johnson R L, Kowalski B J, Kopalko K, Orlowski B A, Kovalyuk Z D and Lashkarev G V 2003 *Phys. Rev. B* **68** 125304
- [34] Yu S-W, Müller N, Heinzmann U, Pettenkofer C, Klein A and Blaha P 2004 *Phys. Rev. B* **69** 045320
- [35] Schlüter M 1973 *Il Nuovo Cimento* **13 B** 313
- [36] Schlüter M, Camassel J, Kohn S, Voitchovsky J P, Shen Y R and Cohen M L 1976 *Phys. Rev. B* **13** 3534
- [37] Doni E, Girlanda R, Grasso V, Balzarotti A and Piacentini M 1979 *Il Nuovo Cimento* **51 B** 154-180
- [38] Klein A, Lang O, Schlaf R, Pettenkofer C and Jaegermann W 1998 *Phys. Rev. Lett.* **80** 361
- [39] Adams J A, Bostwick A, Ohta T, Ohuchi F S and Olmstead M A, 2004 (*submitted to Phys. Rev. B.*)
- [40] Gomes da Costa P, Dandrea R G, Wallis R F and Balkanski M 1993 *Phys. Rev. B* **48** 14135-14141
- [41] Klein A, Tiefenbacher S, Eyert V, Pettenkofer C and Jaegermann W 2001 *Phys. Rev. B* **64** 205416
- [42] Albe K and Klein A 2002 *Phys. Rev. B* **66** 073413
- [43] Harrison W A 1989 *Electronic Structure and the Properties of Solids* (New York: Dover Publications)
- [44] Hoffmann R 1989 *A Chemist's View of Bonding in Extended Structures* (Weinheim: VCH)
- [45] Northrup J A, Bringans R D, Uhrberg R I G, Olmstead M A and Bachrach R Z 1988 *Phys. Rev. Lett.* **61** 2957